

Comparison of Isolobal Fragments: Photoelectron Spectra and Molecular Orbital Calculations of (Arene)tricarbonylchromium, -molybdenum, and -tungsten Complexes

Brien P. Byers and Michael B. Hall*

Department of Chemistry, Texas A&M University, College Station, Texas 77843-3255

Received February 5, 1987

Gas-phase ultraviolet photoelectron spectra (PES) and parameter-free Fenske-Hall molecular orbital (MO) calculations are reported for the following complexes: $(\eta^6\text{-C}_6\text{H}_6)\text{M}(\text{CO})_3$, $(\eta^6\text{-1,3,5-C}_6\text{H}_3(\text{CH}_3)_3)\text{M}(\text{CO})_3$, and $(\eta^6\text{-C}_6(\text{CH}_3)_6)\text{M}(\text{CO})_3$, where M = Cr, Mo, or W. The two most important bonding interactions between the arene ring and metal fragment give rise to two e-type MO's of the $(\pi\text{-arene})\text{M}(\text{CO})_3$ complex. The calculations and PES show that the most stable e MO increases in stability relative to the free ligand on progressive methylation of the benzene ring and on substituting the metal atom in the order Mo < Cr << W. The calculations and PES also show that the second e MO decreases in stability on progressive methylation of the benzene ring and on substituting the metal atom, but now the order is W < Cr < Mo. An analysis of the spin-orbit splitting of the first band in the PES of the tungsten complexes indicates that the metal a_1 MO is above the metal e MO in the benzene complex but below it in the hexamethylbenzene complex. The experimental results show that substitution of the metal atom is a much more important effect in causing the arene ring distortion observed in the low-temperature X-ray crystal structures of these species.

Introduction

Low-temperature X-ray crystallographic studies of $(\text{C}_6\text{H}_6)\text{Cr}(\text{CO})_3$,¹ $(\text{C}_6(\text{CH}_3)_6)\text{Cr}(\text{CO})_3$,² (Figure 1), and $(\text{C}_6\text{-}(\text{CH}_3)_6)\text{Mo}(\text{CO})_3$ ³ have shown a pattern of alternating long and short C-C bonds in the complexed arene ring. It has been determined that substitution of the metal atom is a more important effect than substitution of the arene ring in causing the arene ring distortion.² A previous theoretical study indicated that this interruption of aromaticity should be present in all $(\text{polyene})\text{M}(\text{CO})_m$ complexes when the CO group eclipse polyene C-C bonds.⁴ Theoretical studies also indicate that the observed bond alternation is due to electronic effects, arising from the interaction of the arene ring with the metal tricarbonyl fragment, and is not caused by crystal packing forces.^{4,5}

Ultraviolet photoelectron spectroscopy (PES) is an effective experimental tool in probing the electronic structure of molecules in the valence region⁶ and is used in this work to examine the $\pi\text{-arene-M}(\text{CO})_3$ interaction. The first PES study of $(\pi\text{-arene})\text{M}(\text{CO})_3$ complexes, carried out by Hillier et al.,⁷ combined ab initio molecular orbital (MO) calculations and PES on $(\text{C}_6\text{H}_6)\text{Cr}(\text{CO})_3$. (Benzene = C_6H_6 , 1,3,5-trimethylbenzene = Tmb, and hexamethylbenzene = Hmb.) Subsequent to Hillier's PES and MO study, several PES studies of $(\text{Tmb})\text{M}(\text{CO})_3$ (M = Cr, Mo, W) complexes have appeared.⁸ The PES studies indicate that the bonding is similar in both the C_6H_6 and Tmb species. A qualitative picture of the bonding in $(\text{C}_6\text{H}_6)\text{Cr}(\text{CO})_3$ has

been established by this work.⁹

In this study the PES and Fenske-Hall MO calculations¹⁰ of all nine $(\pi\text{-arene})\text{M}(\text{CO})_3$ (arene = C_6H_6 , Tmb, Hmb; M = Cr, Mo, W) complexes are reported in order to analyze the bonding over the entire series. The changes in ionization potential (IP) of the first two bands in the PES are analyzed to determine the changes in electronic structure, and these changes are related to the trend in arene ring distortion observed in the low-temperature X-ray crystal structure of three of the complexes.¹⁻³

Experimental and Theoretical Details

Synthetic Procedures. All manipulations were carried out under an inert atmosphere of N_2 or Ar. $\text{Cr}(\text{CO})_6$, $\text{Mo}(\text{CO})_6$, and $\text{W}(\text{CO})_6$ were purchased from Pressure Chemical Co.; hexamethylbenzene was purchased from Aldrich Chemical Co. All solids were purified by sublimation in vacuo prior to use. All solvents and liquid reagents were purchased from either Fischer Scientific or Aldrich Chemical Co. and distilled from sodium benzophenone ketyl under an inert atmosphere of N_2 or Ar immediately prior to use. The preparation of all complexes under study have been reported earlier. $(\text{C}_6\text{H}_6)\text{Cr}(\text{CO})_3$, $(\text{Tmb})\text{Cr}(\text{CO})_3$, $(\text{Hmb})\text{Cr}(\text{CO})_3$, $(\text{Tmb})\text{Mo}(\text{CO})_3$, $(\text{Hmb})\text{Mo}(\text{CO})_3$, $(\text{C}_6\text{H}_6)\text{W}(\text{CO})_3$, and $(\text{Tmb})\text{W}(\text{CO})_3$ were all prepared by the method of Mahaffy and Pauson,¹¹ reaction of a 1:1 molar ratio of the metal hexacarbonyl and arene in 120 mL of dibutyl ether and 5 mL of THF. $(\text{C}_6\text{H}_6)\text{Mo}(\text{CO})_3$ was prepared by reaction of $(\text{C}_5\text{H}_5\text{N})_3\text{Mo}(\text{CO})_3$ ¹² with benzene in the presence of $\text{BF}_3\cdot\text{O}(\text{C}_2\text{H}_5)_2$.¹³ $(\text{Hmb})\text{W}(\text{CO})_3$ was prepared by reacting $(\text{CH}_3\text{CN})_3\text{W}(\text{CO})_3$ ¹⁴ with hexamethylbenzene in decane.¹⁵ The products were purified by sublimation in vacuo or by recrystallization from a benzene-hexane mixture in the case of the molybdenum complexes and $(\text{Hmb})\text{W}(\text{CO})_3$. The $(\pi\text{-arene})\text{M}(\text{CO})_3$ complexes were characterized by infrared spectroscopy in the carbonyl region.¹⁶

(1) Rees, B.; Coppens, P. *Acta Crystallogr., Sect. B: Struct. Crystallogr. Cryst. Chem.* 1973, B29, 2515.

(2) Byers, B. P.; Hall, M. B. *Inorg. Chem.* 1987, 26, 2186.

(3) Chesick, J. P.; Koshland, D. E.; Myers, S. E. *Acta Crystallogr., Sect. B: Struct. Crystallogr. Cryst. Chem.* 1977, B33, 2013.

(4) Chinn, J. W.; Hall, M. B. *J. Am. Chem. Soc.* 1983, 105, 4930.

(5) Hoffmann, R.; Albright, T. A. *J. Am. Chem. Soc.* 1977, 99, 7546.

(6) (a) Green, J. C. *Struct. Bonding (Berlin)* 1981, 43, 46. (b) Cowley, A. H. *Prog. Inorg. Chem.* 1979, 26, 46. (c) Rabalais, J. W. *Principles of Ultraviolet Photoelectron Spectroscopy*; Wiley: New York, 1977. (d) Eland, J. H. D. *Photoelectron Spectroscopy*, 2nd ed.; Butterworths: London, 1984.

(7) Hillier, I. H.; Guest, M. F.; Higginson, B. R.; Lloyd, D. R. *Mol. Phys.* 1975, 29, 113.

(8) (a) Kobayashi, H.; Kobayashi, M.; Kaizu, Y. *Bull. Chem. Soc. Jpn.* 1975, 48, 1222. (b) Gower, M.; Kane-Maguire, L. A. P.; Maier, J. P.; Sweigart, D. A. *J. Chem. Soc., Dalton Trans.* 1977, 316. (c) Worley, S. D.; Webb, T. R. *J. Organomet. Chem.* 1980, 192, 139.

(9) (a) Meutterties, E. L.; Bleeke, J. R.; Wucherer, E. J.; Albright, T. A. *Chem. Rev.* 1982, 82, 499. (b) Albright, T. A. *Acc. Chem. Res.* 1982, 15, 149.

(10) Hall, M. B.; Fenske, R. F. *Inorg. Chem.* 1972, 11, 768.

(11) Mahaffy, C. A. L.; Pauson, P. L. *Inorg. Synth.* 1979, 19, 154.

(12) Hieber, W.; Muhlbauer, F. Z. *Anorg. Allg. Chem.* 1935, 221, 337.

(13) Nesemeyanov, A. N.; Krivykh, V. V.; Kaganovich, V. S.; Rybinskaya, M. I. *J. Organomet. Chem.* 1975, 102, 185.

(14) (a) King, R. B.; Fonzaglia, A. *Inorg. Chem.* 1966, 5, 1837. (b) Tate, D. P.; Knipple, W. R.; Augl, J. M. *Inorg. Chem.* 1962, 1, 433.

(15) Doxsee, K. M.; Grubbs, R. H.; Anson, F. C. *J. Am. Chem. Soc.* 1984, 106, 7819.

(16) (a) Brown, D. A.; Hughes, F. J. *J. Chem. Soc. A* 1968, 1519. (b) Parker, D. J.; Stiddard, M. H. B. *J. Chem. Soc. A* 1968, 2263.

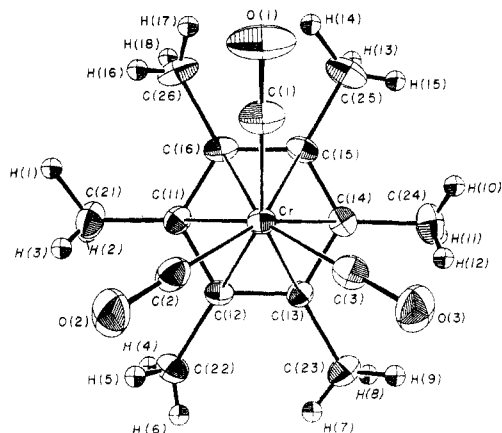


Figure 1. ORTEP plot of the structure of $(\eta^6\text{-C}_6\text{(CH}_3)_6\text{)Cr(CO)}_3$ looking down the pseudo-threefold axis which is assigned as the z axis in our coordinate system.

Photoelectron Spectroscopy. The photoelectron spectra were all recorded on a Perkin-Elmer Model PS-18 spectrometer. The total spectrum of each complex was recorded as a single slow scan. The Ar $2\text{P}_{3/2}$ and $2\text{P}_{1/2}$ lines at 15.76 and 15.94 eV, respectively, were used as an internal reference. The resolution for all spectra was better than 40 meV for the fwhm of the $2\text{P}_{3/2}$ peak. To correct for nonlinearity, the IP of the free benzene e_{1g} orbital at 9.241 eV¹⁷ was used to calibrate the lower energy region of the scale. For the Cr and W complexes no spike was observed at 14 eV, which would correspond to free CO and complex decomposition. However, some decomposition was observed for all Mo complexes; $(\text{C}_6\text{H}_5)_3\text{Mo(CO)}_3$ showed the greatest decomposition and apparently is the least thermally robust complex of the nine studied.

Molecular Orbital Calculations. (a) Method. Fenske-Hall¹⁰ molecular orbital calculations were carried out on all nine $(\pi\text{-arene})\text{M(CO)}_3$ complexes under study. Fenske-Hall calculations are a self-consistent field (SCF), parameter-free type of calculation, the results of which depend only on the atomic basis set chosen and the internuclear distances used. These calculations have been used in the past primarily in a qualitative manner to analyze trends over a series of analogous complexes.¹⁸ Calculations were first performed on the arene and M(CO)_3 fragments separately, and then the converged atomic wave functions for the entire molecule were transformed to the molecular orbital basis of these fragments.

(b) Geometry. The bond lengths used in these calculations were chosen on the basis of the low-temperature X-ray crystal structures of $(\text{C}_6\text{H}_5)_3\text{Cr(CO)}_3$,¹ $(\text{Hmb})\text{Cr(CO)}_3$,² and $(\text{Hmb})\text{Mo(CO)}_3$.³ The arene rings were treated as regular hexagons with D_{6h} symmetry. The M(CO)_3 fragments were taken to have C_{3v} symmetry. The symmetry of all $(\pi\text{-arene})\text{M(CO)}_3$ complexes in the calculations was C_{3v} . The hydrogen atoms attached to ring carbons and methyl group carbons were considered to be in the same plane as the arene ring. The arene ring center to metal atom to carbonyl carbon angle was taken to be 123° .¹⁹ For the C_6H_5 and Hmb species, the M-CO bonds eclipse C-C bonds of the arene ring in the calculations. For the Tmb complexes, the M-CO bonds eclipse carbon atoms of the arene ring with attached methyl groups. The bond distances used are presented in Table I.

(c) Basis Set. For C and O, double- ζ representations for the 2s and 2p orbitals, generated by Bursten and Fenske,²⁰ were used in all calculations. An exponent of 1.16 was used for the 1s orbital of hydrogen. To generate an acceptable basis set which follows

(17) (a) Åbrinsk, L.; Lindholm, E.; Edqvist, O. *Chem. Phys. Lett.* **1970**, *5*, 609. (b) Potts, A. W.; Price, W. C.; Streets, D. G.; Williams, T. A. *Discuss. Faraday Soc.* **1973**, *54*, 168.

(18) (a) Lichtenberger, D. L.; Fenske, R. F. *Inorg. Chem.* **1976**, *15*, 2015. (b) Morris-Sherwood, B. J.; Kolthammer, B. W. S.; Hall, M. B. *Inorg. Chem.* **1981**, *20*, 2771. (c) Chesky, P. T.; Hall, M. B. *Inorg. Chem.* **1983**, *22*, 2998, 3327. (d) Powell, C. B.; Hall, M. B. *Inorg. Chem.* **1984**, *23*, 4619.

(19) Elian, M.; Hoffmann, R. *Inorg. Chem.* **1975**, *14*, 1058.

(20) (a) Fenske, R. F.; Bursten, B. E. *J. Chem. Phys.* **1977**, *67*, 3138. (b) Fenske, R. F.; Bursten, B. E.; Jensen, R. J. *J. Chem. Phys.* **1978**, *68*, 3320.

Table I. Bond Lengths (Å) Used in Fenske-Hall Calculations

	Bz	Tmb	Hmb
Arene Ring ^a			
$C_{\text{ring}}\text{-}C_{\text{ring}}$	1.4080	1.4188	1.4228
Metal - Ring Center			
Cr	1.727	1.729	1.731
Mo, W	1.900	1.908	1.923

Cr

Mo, W

M(CO)_3 ^b

M-C

1.84

1.95

^a For all metals, $C_{\text{ring}}\text{-}C_{\text{methyl}} = 1.50$ Å and $\text{C-H} = 1.10$ Å. ^b For all metals, $\text{C-O} = 1.15$ Å.

Table II. Values Relating to Fenske-Hall Calculations on M(CO)_6 Species

metal	IP $t_{1u}(\text{M(CO)}_6)$ ^a	exp(s,p)
Cr	13.38	2.247
Mo	13.33	2.435
W	13.27	2.797

^a Literature²² and calculated values correspond.

observed trends for the group 6 transition metals, the following procedure was used. The program of Herman and Skillman²¹ was used to generate numerical representations of atomic orbital wave functions. The Herman-Skillman approximation gives wave functions that are reasonably good approximations to Hartree-Fock wave functions. All metal atoms were assumed to be in the M^{1+} and d^5s^0 configuration for the Herman-Skillman calculations. For tungsten, the calculations were corrected for relativistic effects. The output of the Herman-Skillman program was then used as input for the basis program of Bursten and Fenske²⁰ to generate an atomic orbital basis set. In this study, the core atomic orbitals up to the nd orbital were represented by a single- ζ function, the nd orbital by a double- ζ function, and the $(n+1)s$ and $(n+1)p$ orbitals by single- ζ functions. For the outer s and p orbital exponent, the same radial form of the Slater-type orbital (STO) was used:

$$\psi_{s,p} = r^{n-1}e^{-\alpha r}$$

To choose a reasonable exponent (α), we varied the exponent until the $8t_{1u}$ orbital energy of M(CO)_6 matched the corresponding IP. This orbital was chosen because its energy is well-separated from the other IP's and is dominated by the interaction of the outer p orbital with the carbonyl "lone pairs". The $8t_{1u}$ IP's and exponents for the M(CO)_6 species are listed in Table II.

Molecular Orbital Calculations

An MO interaction diagram for $(\text{Hmb})\text{W(CO)}_3$, drawn from the results of the Fenske-Hall MO calculation, is presented in Figure 2. If one compares Figure 2 to an MO diagram for $(\text{C}_6\text{H}_5)_3\text{Cr(CO)}_3$,⁹ one finds that the bonding in these two species is quite similar and that Figure 2 may be used as a representative MO diagram for all complexes in this study. These complexes differ, however, in the energetic placement of the molecular orbitals and electron populations, as will be shown below.

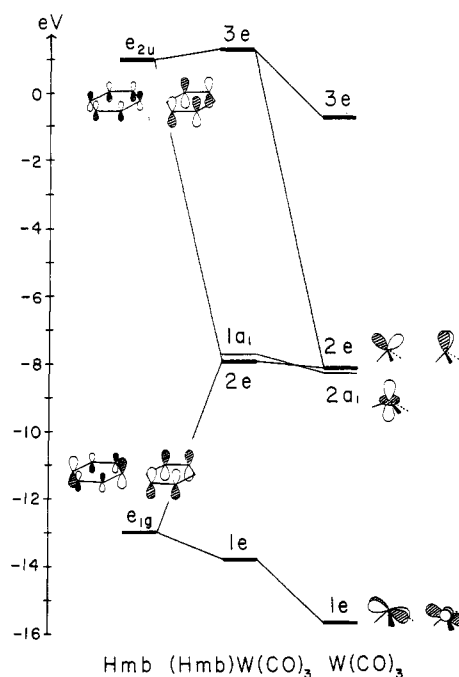
The MO diagram of Figure 2 is constructed from the arene and M(CO)_3 fragments. The M(CO)_3 fragment orbitals most involved in bonding with the arene are those labeled 3e, 2e, 2a₁, and 1e. Presented in Table III are the results of Fenske-Hall calculations¹⁰ on Cr(CO)_3 , Mo(CO)_3 , and W(CO)_3 . For each M(CO)_3 fragment, the metal character of the LUMO 3e is entirely d_π . ($d_\pi = \text{combina-}$

(21) Herman, F.; Skillman, S. *Atomic Structure Calculations*; Prentice-Hall: Englewood Cliffs, NJ, 1963.

(22) Higginson, B. R.; Lloyd, D. R.; Burroughs, P.; Gibson, D. M.; Orchard, A. F. *J. Chem. Soc., Faraday Trans. 2* **1973**, 1659.

Table III. Orbital Energies and Percent Character of the Valence Orbitals of M(CO)₃ Fragments

orbital	energy	metal			carbonyl				
		d _z	d _π	z ²	s	p	4σ	5σ	2π
(a) Cr(CO) ₃									
3e	-0.95		37.50			17.69		5.02	36.88
2e	-6.73	50.42	16.40						31.38
2a ₁	-6.86			62.40					34.77
1e	-14.00	9.24	19.34			5.82	2.72	63.05	
1a ₁	-15.92				6.22		7.98	82.03	
(b) Mo(CO) ₃									
3e	-0.74		27.66			22.88		4.12	42.47
2e	-7.60	47.92	17.80						31.92
2a ₁	-7.68			62.84					34.00
1e	-15.06	9.12	18.56			2.33	5.75	62.79	
1a ₁	-15.72				7.25		6.12	82.96	
(c) W(CO) ₃									
3e	-0.80		23.52			19.78		3.0	51.59
2e	-7.32	45.50	16.90						35.07
2a ₁	-7.34			58.95					37.61
1e	-14.99	8.76	17.78			2.04	6.80	63.18	
1a ₁	-16.07				12.13		9.18	76.02	

Figure 2. Molecular orbital diagram for (Hmb)W(CO)₃. This diagram is representative of all (arene)M(CO)₃ interaction diagrams.

tion of $d_{x^2-y^2}$ and d_{xy} , and d_{π} = combination of d_{xz} and d_{yz} .) The percent d_{π} in the 3e orbital decreases on descending the triad, while the percent of CO 2π increases. The HOMO 2e is composed of >45% d_z and >16% d_{π} , as well as >31% CO 2π character. (The 2e orbital of $M(CO)_3$ is the 10e orbital in the study of Chinn and Hall.⁴) In the 2e orbital the percent d_z character decreases in descending the triad, and the percent CO 2π increases. The percent d_{π} is highest for Mo and lowest for Cr. The total percent metal character decreases from Cr to Mo to W. The 2e and 2a₁ orbitals are nearly degenerate in the $M(CO)_3$ fragments; they are separated by 0.13 eV in $Cr(CO)_3$, 0.08 eV in $Mo(CO)_3$, and 0.02 eV in $W(CO)_3$. The 2a₁ orbital is composed of ~60% metal d_{z^2} character and >34% carbonyl 2π character; $Mo(CO)_3$ has the most metal and least CO character, and $W(CO)_3$ has the least metal and most CO character. The 1e orbital of $M(CO)_3$, separated from the 2e and 2a₁ orbitals by ~7 eV, is mostly carbonyl 5σ in character, ~63% for each fragment. The 1e orbital

Table IV. Mulliken Populations of M(CO)₃ and Arene Ring Fragments

	M(CO) ₃		arene	
	2e	3e	e _{1g}	e _{2u}
(Bz)Cr(CO) ₃	1.786	0.143	1.878	0.200
(Tmb)Cr(CO) ₃	1.799	0.151	1.864	0.175
(Hmb)Cr(CO) ₃	1.813	0.161	1.853	0.170
(Bz)Mo(CO) ₃	1.789	0.137	1.873	0.184
(Tmb)Mo(CO) ₃	1.808	0.142	1.861	0.164
(Hmb)Mo(CO) ₃	1.827	0.147	1.848	0.145
(Bz)W(CO) ₃	1.760	0.111	1.880	0.213
(Tmb)W(CO) ₃	1.788	0.110	1.873	0.194
(Hmb)W(CO) ₃	1.803	0.125	1.857	0.169

also contains ~18% d_{π} , ~8% d_z , and a small amount of carbonyl 4σ character. For the 1e orbital the percent metal character decreases, while the percent of CO σ character increases, on descending the triad.

At the left of Figure 2 are the two sets of doubly degenerate e orbitals of the arene: the e_{1g} (HOMO) and the e_{2u} (LUMO). At the far right of Figure 2 are drawings of the five metal d orbitals. It is apparent from Figure 2 that the 2e orbital, which is mostly $d_{x^2-y^2}$ and d_{xy} (d_z), will interact most strongly with the e_{2u} orbitals of the arene. The 1e orbital, which is mostly d_{xz} and d_{yz} (d_{π}), will interact with the e_{1g} orbitals, as will the $M(CO)_3$ 3e orbital, which has only d_{π} metal character. The near degeneracy of the 1e $M(CO)_3$ and arene e_{1g} orbitals cause them to mix, but since they are both occupied, no net bonding results from this mixing. The orbitals of the (π -arene) $M(CO)_3$ complexes, shown in Figure 2, are constructed as follows: the HOMO 1a₁ is nearly all $M(CO)_3$ 2a₁, the SHOMO 2e is mostly $M(CO)_3$ 2e (~85%) but contains some arene e_{2u} (~8%), and the 1e orbital is mostly arene e_{1g} (~70%) but also has some associated $M(CO)_3$ 1e and 3e character (~30%). The 2e-e_{2u} interaction represents metal to arene donation (back-bonding), while the e_{1g}-3e interactions represents arene to metal donation. It should be noted that the $M(CO)_3$ 2e orbital is made up of a significant amount (>30%) of carbonyl 2π character. Although the possibility of a through-space interaction of the carbonyls with the arene was raised by Chinn and Hall,⁴ an ab initio deformation density study of $(C_6H_6)Cr(CO)_3$ by Kok and Hall²³ showed no significant direct interaction of the carbonyls and the benzene ring.

(23) Kok, R. A.; Hall, M. B. *J. Am. Chem. Soc.* 1985, 107, 2599.

Table V. Percent Character of (π -Arene) $M(CO)_3$ Complexes^a

	MO	energy	2a ₁	M(CO) ₃		arene	
				2e	3e	e _{1g}	e _{2u}
(Bz)Cr(CO) ₃	1a ₁	-8.24	99.58				
	2e	-8.61		86.16	1.97	1.25	9.19
	1e	-15.25		2.75	5.50	90.61	
(Tmb)Cr(CO) ₃	1a ₁	-7.84	99.65				
	2e	-8.04		85.94	2.19	1.60	8.04
	1e	-14.52		3.06	5.52	89.48	
(Hmb)Cr(CO) ₃	1a ₁	-7.65	99.64				
	2e	-7.91		86.77	2.29	1.67	7.82
	1e	-13.65		2.75	6.17	88.14	
(Bz)Mo(CO) ₃	1a ₁	-8.66	99.06				
	2e	-8.96		84.38	2.81	2.95	8.53
	1e	-15.38		4.09	4.55	89.82	
(Tmb)Mo(CO) ₃	1a ₁	-8.39	98.93				
	2e	-8.74		85.87	2.99	2.58	7.76
	1e	-14.52		3.55	4.97	89.49	
(Hmb)Mo(CO) ₃	1a ₁	-8.14	98.94				
	2e	-8.29		85.07	3.09	3.46	6.71
	1e	-13.78		4.95	4.97	87.01	
(Bz)W(CO) ₃	1a ₁	-8.37	99.12				
	2e	-8.70		83.12	2.55	2.45	9.92
	1e	-15.52		3.85	3.93	90.10	
(Tmb)W(CO) ₃	1a ₁	-8.12	98.98				
	2e	-8.50		84.74	1.81	1.81	9.04
	1e	-14.67		3.38	4.20	89.90	
(Hmb)W(CO) ₃	1a ₁	-7.89	99.00				
	2e	-8.05		84.19	2.78	3.30	7.84
	1e	-13.92		4.64	4.22	86.97	

^aThe 1e molecular orbital of the (arene) $M(CO)_3$ molecule has been localized on the benzene ring to remove the near-degenerate mixing of this orbital with the 5 σ carbonyls (1e of $M(CO)_3$).

Tables IV and V illustrate how the complexes change as the substitutions occur. Table IV lists the Mulliken populations²⁴ for the arene and $M(CO)_3$ fragment orbitals of the (π -arene) $M(CO)_3$ complexes. Table V lists the energies and percent character of molecular orbitals as determined by the Fenske-Hall calculations. The Mulliken populations show several trends concerning the changes in bonding in the complexes as the central metal atom or arene ring is changed. The Mulliken populations for the arene ring show that the HOMO e_{1g} is occupied by less than two electrons (1.85–1.88) and that the LUMO e_{2u} is slightly occupied (0.16–0.21). For the same metal atom, the populations of both the e_{1g} and e_{2u} orbitals decrease as follows: C₆H₆ > Tmb > Hmb. For the same arene, but different metal atoms, the populations decrease as follows: W > Cr > Mo. Table IV also lists the Mulliken populations for two orbitals of the $M(CO)_3$ fragment. The Mulliken populations of the 2a₁ and 1e orbitals have not been included because these orbitals have little involvement in the arene– $M(CO)_3$ bond, and the populations are constant over the series of complexes. The Mulliken population of the 3e orbital of the $M(CO)_3$ fragment increases when C₆H₆ is substituted with Tmb and then with Hmb and decreases when Cr is substituted with Mo and then with W. The 2e orbital of the $M(CO)_3$ fragment (which interacts with the arene e_{2u}) shows the same trend as the 3e orbital; substitution of the arene, with the same metal atom, causes an increase in the populations as follows: C₆H₆ < Tmb < Hmb. However, the 2e orbital population shows a different trend when substituting the metal atom for the same arene: Mo > Cr > W.

Table V lists the energies and percent character of the three most important orbitals of the (π -arene) $M(CO)_3$ complexes. There are several differences between the C₆H₆, Tmb, and Hmb complexes. For the same metal

atom, the 1e orbital of the complex has slightly more $M(CO)_3$ 3e and less arene e_{1g} character in going from C₆H₆ to Tmb to Hmb. Like the 1e orbital, the 2e orbital remains fairly constant in composition for all species, but it does contain slightly less arene e_{2u} character in going from C₆H₆ to Tmb to Hmb. The 1a₁ orbital of the complex is ~99% of $M(CO)_3$ 2a₁ in character for every complex. As expected, the calculations show that for each metal, the energies of each orbital become progressively higher as methyl substitution increases. The calculations also predict that the 1a₁ and 2e MO's move in the same direction; both becoming less stable for more highly substituted arenes. Differences between complexes with the same arene ring but different metal atom may also be seen in Table V. The stability of the 1e MO shows a periodic trend: W > Cr > Mo. However, the 2e MO does not display a periodic trend for the orbital energy, decreasing in energy as follows: Cr > W > Mo.

Several explanations as to the occurrence of long-short C–C bond alternation in (π -arene) $M(CO)_3$ complexes have been offered.⁹ One explanation involves the $M(CO)_3$ fragment accepting electron density from the C–C π bond, which the CO group eclipses, thereby reducing the π -electron density in the bond. Another explanation is that the carbonyls and metal atom form hybrid orbitals trans to the CO groups and cause the π bonds to localize in the region of the hybrid orbitals. The first explanation emphasizes effects of CO π bonding, while the second emphasizes the effects of CO σ bonding. It has been suggested^{4,5} that the arene ring distortion is caused by a mixing of the antibonding arene e_{2u} and bonding e_{1g} orbitals, in the bond with the $M(CO)_3$ 2e orbital. In the threefold symmetry of the (π -arene) $M(CO)_3$ complexes both the e_{1g} and e_{2u} orbitals of the arene are of e symmetry and their mixing would provide bond alternation. The mixing seems to be driven by the $M(CO)_3$ fragment 2e orbital. Table V shows that the percentages are small, but the Hmb complexes have a more equal mixture of arene e_{1g} and e_{2u} orbitals than the C₆H₆ species. For changing the metal atom, the percentage of arene orbitals becomes more equal on the order Cr < W < Mo. One might expect to see the W and Mo complexes reversed, but the values for W and Mo are nearer each other than either are to Cr.

The direction of the slight change in the Mulliken populations indicates that for the same metal atom, a slightly stronger interaction between the 3e and e_{1g} orbital is present in going from C₆H₆ to Tmb to Hmb. The increased electron donation by the arene arise because the arene's e_{1g} orbitals gets closer in energy to the metal orbital as the methyl substitution increases. Table IV also indicates that for the same arene, the 3e–e_{1g} interaction is lessened when the triad is descended. Thus, the $W(CO)_3$ fragment is the poorest electron acceptor. The decrease in e_{2u} population and increase in the 2e population is due to the increase in the energy difference between the arene e_{2u} and $M(CO)_3$ 2e MO. A lessening of e_{2u}–2e interaction in the series C₆H₆, Tmb, and Hmb is also supported by Table V; the percent of e_{2u} character in the complex's 2e MO decreases from C₆H₆ to Tmb to Hmb. The populations of both the e_{1g} and e_{2u} orbitals indicate that the $Mo(CO)_3$ species are the best electron acceptors but the poorest electron donors. The population of the 2e $M(CO)_3$ orbital supports the idea that the Mo fragment is the poorest donor to the arene, but the population of the 3e orbital suggest that the $Cr(CO)_3$ is a better electron acceptor than $Mo(CO)_3$.

It is concluded from the calculations that the 1e MO is more stabilized in going from C₆H₆ to Tmb to Hmb be-

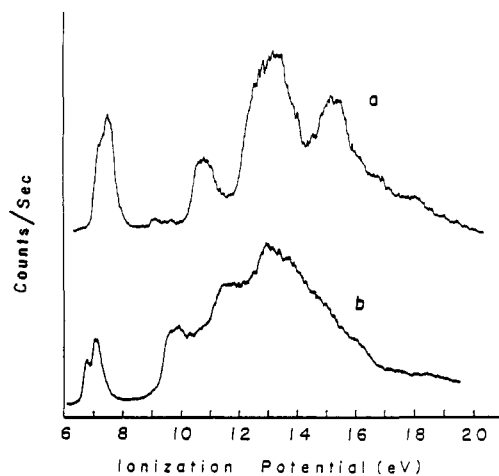


Figure 3. Ultraviolet photoelectron spectra of $(C_6H_6)W(CO)_3$ and $(Hmb)W(CO)_3$ are shown in a and b, respectively.

cause of more electron donation from the arene ring in a stronger $M(CO)_3$ 3e-arene e_{1g} interaction. The $M(CO)_3$ 2e-arene e_{2u} interaction is probably weaker in going from C_6H_6 to Tmb to Hmb due to the larger energy difference between the two orbitals and increasingly poorer acceptor ability of the arene. More mixing of arene e_{1g} and e_{2u} orbitals is seen for the Hmb complexes than for the C_6H_6 complexes. By progressively substituting Cr by Mo and W the metal levels first become more stable than less stable (orbital stability $Mo > Cr > W$). Thus, Mo is the poorest electron donor to the arene and to the carbonyls. On the other hand the arene donates more to Mo than to the other metals. The calculations do not allow one to predict unambiguously which effect (arene ring or metal substitution) is more important in causing arene ring distortion.

Photoelectron Spectroscopy

Shown in Figure 3 are the full photoelectron spectra of $(C_6H_6)W(CO)_3$ and $(Hmb)W(CO)_3$. The first band for both spectra in Figure 3 is due to ionizations from the closely spaced $1a_1$ and $2e$ MO's, and the second band is due to ionizations from the $1e$ MO.⁷ The structure past the first two peaks results from ligand ionizations. The PE spectrum of $(C_6H_6)W(CO)_3$ is nearly identical with that of $(C_6H_6)Cr(CO)_3$, reported earlier by Hillier,⁷ with the exception that the first, mostly metal band is split. The splitting of the first band in the PES of $(\pi\text{-arene})W(CO)_3$ complexes was first noticed in the PES of $(Tmb)W(CO)_3$ ⁸ and was attributed to spin-orbit coupling. The PE spectrum of $(Hmb)W(CO)_3$ shows an even greater split than $(C_6H_6)W(CO)_3$ in the first band. The weak feature between the first and second peaks in the PE spectrum of $(C_6H_6)W(CO)_3$ is due to some residual-free benzene. The following discussion will be concerned first with the trends in the ionization potential (IP) of the first, mostly metal d band as well as the origin of the band splitting in the tungsten complexes, in relation to whether or not Koopmans' theorem²⁵ holds for the order of the $1a_1$ and $2e$ MO's. The second part of the discussion will be concerned with trends involving the second band.

Figure 4 is a plot of the measured vertical IP's of the first band in the PE spectra. The data points for all complexes fall (within experimental error) along straight lines. The slope of the lines for the Cr and Mo complexes are very nearly equal. The slope of the lines for the W complexes are somewhat steeper and are separated by 0.23, 0.26, and 0.30 eV on going from C_6H_6 to Tmb to Hmb.

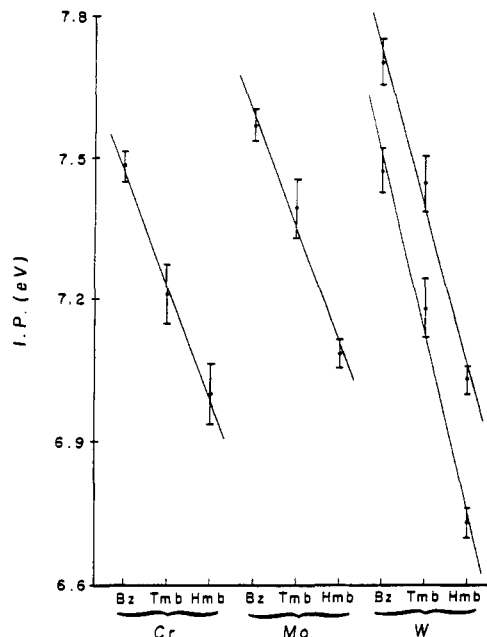


Figure 4. Plot of the ionization energies for the first, primarily metal, band in the PES.

Figure 4 indicates that the metal d band is becoming less stable on going from the C_6H_6 to the Hmb complex. The destabilization of the first band is due to an increase in the energy of the arene MO's in going from C_6H_6 to Tmb to Hmb. Across this series the arene is becoming a better donor and a poorer acceptor. The metal's energy levels are raised by the larger donation, and the weaker e_{2u} -2e interaction further destabilizes the metal's energy levels. Therefore, for the same metal atom progressive substitution of C_6H_6 by Tmb and Hmb will destabilize the first band in the PES. Figure 4 also illustrates the effect of substituting the metal atom with the same arene from left to right across the figure. Going by the IP of the first ionization of the W complexes, we see that the W IP's are lower than for the Cr or Mo analogues. Figure 4 indicates a nonperiodic trend in the energy of the first band: $W < Cr < Mo$. This is the same trend seen in Table V for the energies of the $1a_1$ and $2e$ orbitals.

The splitting of the first band in the PE spectra of the W complexes has been attributed to spin-orbit coupling⁸ (SOC). An analysis of the SOC in these complexes may be carried out by using a simple molecular orbital model. This model was first developed by M.B.H. for the analysis of SOC in diatomic halogens²⁶ and substituted rhenium pentacarbonyls.²⁷ The model was later used by Lichtenberger and Fenske²⁸ in analyzing SOC for $(Cp)M(CO)_3$ complexes (assumed to have C_{3v} symmetry). From Fenske-Hall calculations on $(\pi\text{-arene})W(CO)_3$ complexes, it's seen that the character of the highest lying a_1 orbital is $\sim 54\%$ metal d, and the e is $\sim 50\%$ metal d. For simplification, we will assume that these orbitals can be represented by the same effective metal d orbital. Thus, in C_{3v} symmetry

$$a_1 = d_{z^2}$$

$$e_x = 0.913d_{xy} + 0.408d_{xz} \quad (1)$$

$$e_y = 0.913d_{x^2-y^2} + 0.408d_{yz}$$

(26) Hall, M. B. *Int. J. Quantum Chem., Symp.* 1975, No. 9, 237.

(27) Hall, M. B. *J. Am. Chem. Soc.* 1975, 97, 2057.

(28) Lichtenberger, D. L.; Fenske, R. F. *J. Am. Chem. Soc.* 1976, 98,

To determine how the e orbital is split by SOC, a pure d orbital interaction matrix is generated.^{26,28} A transformation matrix, with columns representing atomic expansion coefficients of each molecular spin orbital is also generated, and the pure d SOC matrix is transformed to this basis. The SOC matrix generated from eq 1 is as follows:

$$\begin{pmatrix} \langle e_y^+ | \\ \langle e_x^+ | \\ \langle a_1^- | \end{pmatrix} \begin{pmatrix} |e_y^+\rangle \\ |e_x^+\rangle \\ |a_1^-\rangle \end{pmatrix} = \begin{pmatrix} 0 & -0.75i\zeta & -0.35i\zeta \\ 0.75i\zeta & 0 & 0.35\zeta \\ 0.35i\zeta & 0.35\zeta & 0 \end{pmatrix} \quad (2)$$

where $i = (-1)^{l+1/2}$, ζ = the effective spin-orbit coupling parameter, and the + and - superscripts on the MO's refer to electron spins. The block of opposite spin has elements that are the negative of those above. To simplify matters, a change of basis is made to

$$|e'^+\rangle = 1/\sqrt{2}(|e_y^+\rangle - i|e_x^+\rangle)$$

$$|e''^+\rangle = 1/\sqrt{2}(|e_y^+\rangle + i|e_x^+\rangle)$$

The degeneracy of the e orbital is removed by this change of basis. Since the SOC is considered to be a perturbation on the HFR matrix before SOC, HFR matrix with SOC becomes

$$\begin{pmatrix} \langle e'^+ | \\ \langle e''^+ | \\ \langle a_1^- | \end{pmatrix} \begin{pmatrix} |e'^+\rangle \\ |e''^+\rangle \\ |a_1^-\rangle \end{pmatrix} = \begin{pmatrix} E_e - 0.75\zeta & 0 & 0 \\ 0 & E_e + 0.75\zeta & -0.5i\zeta \\ 0 & 0.5i\zeta & E_{a_1} \end{pmatrix} \quad (3)$$

Lichtenberger and Fenske²⁸ calculated from the 0.26-eV splitting observed in the first band of $W(CO)_6$ ²² that $\zeta = 0.18$ eV in this complex. The PES data^{6a} for some bis-(arene)tungsten complexes show the following spin-orbit splittings for the e_{2g} MO: $(C_6H_6)_2W$, 0.43 eV; $(toluene)_2W$, 0.37 eV; $(Tmb)_2W$, 0.35 eV. With use of the model of Lichtenberger and Fenske²⁸ the calculated ζ values for these species are 0.22, 0.19, and 0.18 eV, respectively. It is interesting to note that the ζ value decreases for the substituted arene rings. From the PES data for the bis-(arene) complexes and $W(CO)_6$ it is possible to estimate a ζ value for $(Hmb)W(CO)_3$ of 0.18 eV. From the SOC matrix above it can be seen that under SOC the $2e$ MO is split into e' and e'' states, with the e' state being lower in energy. (The notation is for the appropriate double group.) The energy difference between the e' and e'' states is 1.5ζ or ~ 0.27 eV. The $1a_1$ MO is of e'' symmetry in the double group and so may interact with the other e'' state.

Several questions arise about the effects of SOC: as to the placement in energy of the a_1 and e orbitals relative to each other and the cause of the increased splitting of the first band for $(Hmb)W(CO)_3$ vs. that for $(C_6H_6)W(CO)_3$. A simple semiquantitative model may be constructed that will show where in energy the a_1 and e orbitals lie, with respect to each other. The shape of the first band can be seen in Figure 3; a smaller peak appears first, followed by a larger peak. Figure 5 is a semiquantitative diagram of the splitting observed in $(C_6H_6)W(CO)_3$. The first band is split in this complex by ~ 0.24 eV. Assuming a ζ value for $(C_6H_6)W(CO)_3$ of 0.18 eV, the observed splitting of would be predicted if the a_1 orbital lies above the e in the ground state, by ~ 0.1 eV. As seen in Figure 3, the first band in the PE spectrum of $(Hmb)W(CO)_3$ shows a larger splitting than that in the PE spectrum of $(C_6H_6)W(CO)_3$. Since mixing of metal and ligand character reduces the magnitude of SOC,²⁹ one explanation could be that the $2e$

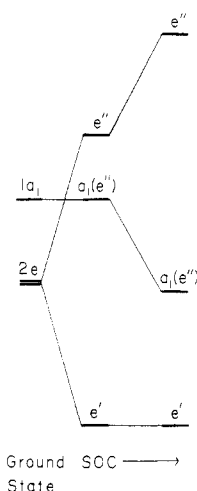


Figure 5. Diagram illustrating the semiquantitative ordering of the $2e$ and $1a_1$ for $(C_6H_6)W(CO)_3$ as determined from the PES.

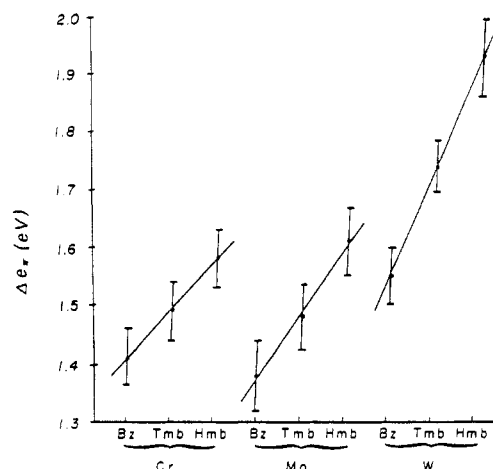


Figure 6. Plot of the change upon complexing of the arene e_π ionization energy.

orbital of $(Hmb)W(CO)_3$ is higher in metal character than the $2e$ orbital of $(C_6H_6)W(CO)_3$. The calculations show that the percent of metal character in the $2e$ MO increases only slightly from the C_6H_6 to the Hmb complex (see Table V). Furthermore, a larger value of ζ for $(Hmb)W(CO)_3$ is not supported by the PES data for bis(arenes).^{6a} The larger splitting could also be caused by the a_1 and e orbital moving closer together in going from $(C_6H_6)W(CO)_3$ to $(Hmb)W(CO)_3$. This effect is seen in the molecular orbital calculations. Table V shows that the calculated energy difference between the a_1 and e orbitals is 0.33 eV for $(C_6H_6)W(CO)_3$ and 0.16 eV for $(Hmb)W(CO)_3$. However, our model would require the a_1 orbital to pass below the e orbital in order to predict the splitting of 0.30 eV observed in the spectrum. Thus, there could be a small deviation in the order of these states from that predicted in this calculation.

The second part of this discussion will be concerned with the change in energy of the free arene e_{1g} orbital on complexation. Figure 6 is a plot of the Δe_π data for each complex. $\Delta e_\pi = (\text{IP of free arene } e_{1g}) - (\text{IP of complex } 1e \text{ MO})$. The data points for the complexes of each metal fall along straight lines. The slope of the line for the Cr and Mo complexes are nearly equal, but the slope for the W complexes is much steeper than the others. This is similar to the effect seen earlier for the first band. One would expect to see an increase in stability for the Hmb complexes over the Tmb and C_6H_6 complexes because CH_3 is an electron-donating group; there should be progressively

(29) Yarbrough, L. W., II; Hall, M. B. *Inorg. Chem.* 1978, 17, 2269.

more electron density available for bonding on going from C₆H₆ to Tmb to Hmb, and the e_{1g} orbital of the arene is closer to the metal in energy. Figure 6 shows progressive stabilization of the 1e with progressive ring methylation; the Hmb complexes are the most stabilized of all. Figure 6 also shows the metal substitution, at least for the W species, is an important effect in stabilizing the e_π orbital of the arene. This much larger stabilization of the W complexes over the Cr or Mo analogues is not seen in the calculations. The straight line plots of Figures 4 and 6 lead one to ask the question: if C–C long-short bond alternation in the arene is dependent on the stability of the MO's of the complex, might (Hmb)W(CO)₃ show even greater ring distortion than (Hmb)Mo(CO)₃?

The PES results show that for the same metal atom the magnitude of Δe_π follows the order (Hmb)M(CO)₃ > (Tmb)M(CO)₃ > (C₆H₆)M(CO)₃ and for the same arene follows the order (π-arene)W(CO)₃ > (π-arene)Mo(CO)₃ ≈ (π-arene)Cr(CO)₃. The PES results also show that the IP of the 2e MO follows a nonperiodic trend, decreasing on the order Mo > Cr > W. The calculated ordering of the 1a₁ MO above the 2e MO is verified by the PES data. Trends in the IR stretching frequencies parallel the trends in the IP's.³⁰ For ν(CO) the trend is Mo > Cr > W for the metals and C₆H₆ > Tmb > Hmb for the arenes. Thermodynamic studies³¹ suggest a small strengthening of the arene–metal bond along the series C₆H₆ < Tmb < Hmb and a large strengthening along the series Cr < Mo < W. The latter differences are larger than one would expect from the changes seen in the PES or IR.

Conclusion

In this work the bonding in the Cr, Mo, and W tricarbonyl complexes of C₆H₆, Tmb, and Hmb has been analyzed. The calculations and PES data agree on the stability of the two most important MO's in these complexes: the 1e and 2e orbitals. The stability of the 1e follows the trend Mo < Cr ≪ W for substituting the metal atom and the trend C₆H₆ < Tmb < Hmb for substituting

the arene ring. For the 2e MO the stability changes to W < Cr < Mo when substituting a metal atom and to Hmb < Tmb < C₆H₆ when substituting the arene ring. A more marked change is seen in the stability of the 1e orbital and in the instability of the 2e orbital when substituting Cr or Mo with W. An analysis of the spin–orbit coupling seen in the W complexes showed that the calculations are correct in assigning the 1a₁ MO above the 2e MO for (C₆H₆)W(CO)₃ but may be incorrect in making the same assignment for the (Hmb)W(CO)₃ since the analysis suggests that the 1a₁ MO is below the 2e MO in this complex. The calculations indicate more arene e_{1g}–e_{2u} mixing for the Hmb over the C₆H₆ complexes and a greater mixing on substituting the metal atom on the order Cr < W < Mo, thus suggesting more C–C bond alternation in the Hmb over the C₆H₆ complexes and more alternation for the heavier metals of the triad. Generally, Mo is the poorest donor of electrons to π-acceptor ligands and the best acceptor of electrons from donor ligands. Thus, as better arene donors are substituted, the stability of the (arene)Mo(CO)₃ complexes increases and they become less susceptible to CO loss.

The low-temperature X-ray crystal structure of (Hmb)Cr(CO)₃ shows that electronic effects and not crystal packing forces cause the observed C–C bond length alternation.² PES data and X-ray crystal structures of (π-arene)M(CO)₃ complexes show substitution of the metal atom is a more important effect in causing arene ring distortion than substitution of the arene ring. The data suggests that further low-temperature X-ray crystallographic studies on these complexes will show that at least some arene ring distortion is present in all of the C₆H₆ and Hmb complexes in this series. If the distortion is related to the strength of the arene–M interaction, the PES data and thermodynamic data would lead us to predict that the W complexes will show the largest distortion. However, if the distortion is related to the degree of mixing of the arene e levels in the primarily metal e band, then Mo with the most stable e IP will show the largest distortion.

Acknowledgment. We thank the Robert A. Welch Foundation (Grant A-648) for the support of this work.

Registry No. (Bz)Cr(CO)₃, 12082-08-5; (Tmb)Cr(CO)₃, 12129-67-8; (Hmb)Cr(CO)₃, 12088-11-8; (Bz)Mo(CO)₃, 12287-81-9; (Tmb)Mo(CO)₃, 12089-15-5; (Hmb)Mo(CO)₃, 12216-16-9; (Bz)W(CO)₃, 12128-53-9; (Tmb)W(CO)₃, 12129-69-0; (Hmb)W(CO)₃, 33505-53-2.

(30) (a) Brown, D. A.; Hughes, F. J. *J. Chem. Soc. A* 1968, 1519. (b) Parker, D. J.; Stiddard, M. H. B. *J. Chem. Soc. A* 1968, 2263.

(31) (a) Connor, J. A.; Skinner, H. A.; Virmani, Y. *J. Chem. Soc., Faraday Trans. 1* 1973, 1218. (b) Brown, D. L. S.; Connor, J. A.; Demain, C. P.; Leury, M. L.; Martinho-Simoes, J. A.; Skinner, H. A.; Moaltar, M. T. Z. *J. Organomet. Chem.* 1977, 142, 321. (c) Nolan, S. P.; de la Vega, R. P.; Hoff, C. D. *J. Organomet. Chem.*, to be submitted for publication.